Figure 5a indicates that the fraction remaining for 60 micron particles in layer 2 (FY) at $t = 1\ s$ and $u = 0.5\ m/s$ is 0.14.

The fractional resuspension rate $\Lambda(t)$ obtained for each layer of a 5-layer deposit is shown in Figure 6. The (top) layer 1 resuspends first and is characterized by the highest rates. Accordingly, all particles at the top layer are unobstructed from above thus free to resuspend as long as it is stochastically possible. However, $\Lambda(t)$ for the layers beneath are substantially dependent on the layer above them, therefore, a different behaviour is observed where $\Lambda(t)$ increases with time. This increase of $\Lambda(t)$ for $t < 10^{-2}$ s is associated with more particles detached from each layer as exposure time increases. As long as the number of detached particles increases from the top layer, the exposed particles at the second layer become more and the resuspension rate increases with time. Accordingly, the same condition applies for particles at layer 3, 4 and 5. Thus, $\Lambda(t)$ at short exposure to the airflow is lower for higher layer number: particles at layers $i \geq 2$ require a short-time period in order to be uncovered. In general, for a thicker deposit it is expected that $\Lambda(t)$ preserves lower rates for higher layer number. Similar findings are reported in Zhang et al. (2013).

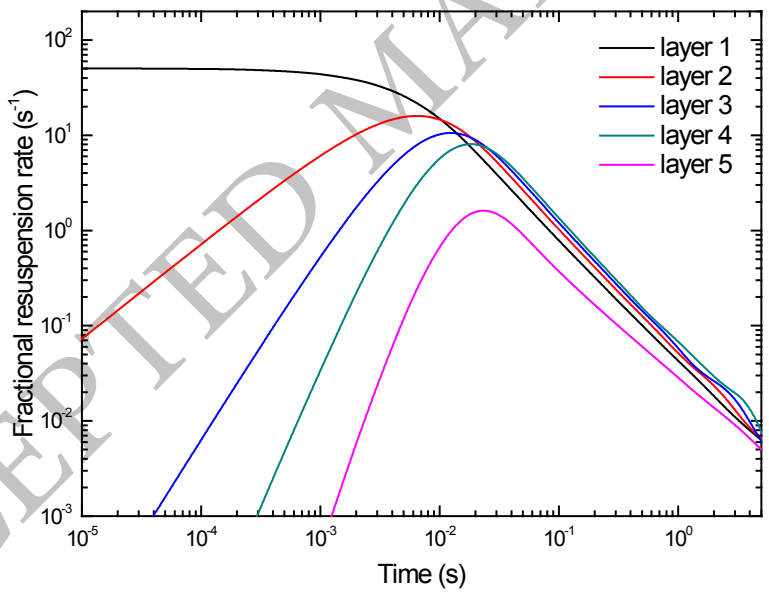

Figure 6: Fractional resuspension rate for each layer of a 5-layer deposit of 60 stainless steel particles on a stainless steel surface versus time at friction 0.4 m/s. The *FY* kinetic was used.

Additionally, Figure 7 presents the total fractional resuspension rate for 3 deposits that differ only in the number of layers. For all three cases $\Lambda(t)$ presents similar rates at a very short exposure time but as t increases $\Lambda(t)$ follows different rates for different deposits. This observation is directly linked with the growth of resuspension within the deposit. At $t < 3 \cdot 10^{-3}\ s$ resuspension takes place only at the first

three layers for all deposits, thus $\Lambda(t)$ preserves similar rates. However, as resuspension moves further into the deposit particles start to detach from layer 4 and $\Lambda(t)$ retains high values for the 5-layer and the 10-layer deposit. On the contrary, $\Lambda(t)$ for the 3-layer deposit (no 4th layer) decreases. The same finding applies for the 5-layer deposit, thus at $t = 10^{-2}\ s$ particle resuspension starts to take place at layer 6 of the 10-layer deposit and the deviation between the two curves is observed. These results match the ones presented by Zhang et al. (2013) and strongly suggest that the fractional resuspension rate preserves higher values as the number of layer increases, i.e. when thicker deposits are involved.

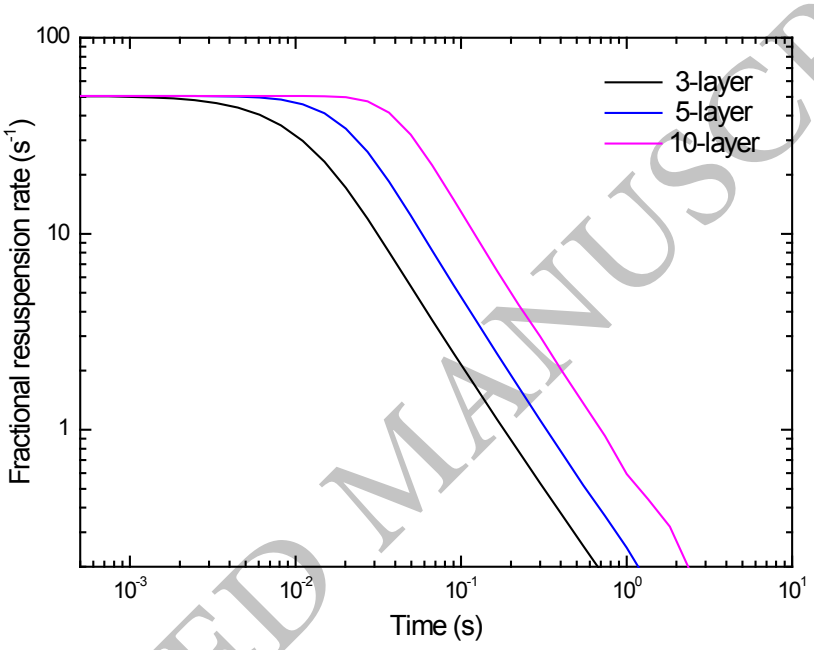

Figure 7: Total fractional resuspension rate for a 3-layer, a 5-layer and a 10-layer deposit composed of 60 stainless steel particles on a stainless steel surface versus time at friction 0.4 m/s. The *FY* kinetic was used.

3.4 Influence of exposure time and the $1/t$ law

Both Figures 6 and 7 demonstrate a relationship of the fractional resuspension rate $\Lambda(t)$ with exposure time to the flow. Accordingly, two regimes are identified: a short-term regime (< 10^{-2} s) where the resuspension rate is high and a long-term regime (> 10^{-2} s), where the resuspension rate decays algebraically with time. Our numerical results are in agreement with previous studies (Reeks et al. 1988; Lazaridis and Drossinos 1998; Reeks and Hall 2001; Friess and Yadigaroglu 2002), where the long-term resuspension rate was found to depend inversely with exposure time. This behaviour is strongly associated with the balance of adhesive and aerodynamic forces (Reeks et al. 1988; Friess and Yadigaroglu 2001;

Benito et al. 2015). At small timescales where the low adhered particles are instantaneously resuspended, the aerodynamic forces are stronger than the adhesive forces and high rates are observed. However, at higher exposure time the fraction of strongly adhered particles on the surface increases and the resuspension rate decreases considerably.

Theoretical predictions (Wen and Kasper 1989; Reeks et al. 1988; Lazaridis et al. 1998; Reeks and Hall 2001; Friess and Yadigaroglu 2002) associate the long-term fractional resuspension rate with the inversely dependence on the exposure time. Indeed, $\Lambda(t)$ decreases linearly with exposure time after a short period corresponding to the short-term regime. The power law that determines the decay of the resuspension rate is in the form:

$$\Lambda(t) = constant\ t^{-\varepsilon} \tag{17}$$

where, ε represents the decay constant. Several authors have suggested that ε corresponds to values close to 1 (Wen and Kasper 1989; Lazaridis et al. 1998; Friess and Yadigaroglu 2002).

Figure 8 presents the fractional resuspension rate versus time for each layer of a 3-layer deposit and plotted at different friction velocities. Using Equation (17) to fit the numerical results of the model, values for ε were derived. Table 2 presents the fitted values of ε applied in Equation (17) for each friction velocity and layer. Our numerical results confirm the power law, although, the values of ε were scattered and usually above 1. Values higher than 1 are also reported in Benito et al. (2015). Hence, the present results indicate that the long-term fractional resuspension rate decays inversely with exposure time but with rates higher than the $1/t$ law. Table 2 also suggests that ε increases with friction velocity for all layers. We found that the decay constant ε increases linearly with friction velocity. The linear increase of ε with friction velocity is associated with enhanced decrease of the fractional resuspension rate at higher friction during long exposures. In other words, a higher ε corresponds to a stronger removal force therefore the slope of the curves maintain higher estimates. A similar characteristic is reported in Benito et al. (2015), where the behaviour of the resuspension flux at long-term regime was associated with the degree of the overlap between the aerodynamic and the adhesive force distributions.

In addition, Figure 8 suggests an inverse of the curves at long-term regime. At short exposure time higher resuspension rates correspond to the layers closer to the flow, $\Lambda_1(t) > \Lambda_2(t) > \Lambda_3(t)$, as a direct consequence of the position of the layer. Particles at layer 1 resuspend with the highest rates since there is no obstacle from above. However, at long-term regime when resuspension has moved further into the deposit this behaviour is inversed and $\Lambda_3(t) > \Lambda_2(t) > \Lambda_1(t)$. Model predictions suggest that more particles detach from bottom layer (expressed by the higher rates), since particles at layer 1 and 2 were resuspended prior to particles at layer 3. Thus $\Lambda(t)$ decreases faster at these two layers. This observation

is not clearly shown in Figure 8a (as well as in Figure 6), but this is due to the decreased removal force represented by $u_* = 0.5\, m/s$, where longer exposure to the flow is needed to obtain the inverse of the curves.

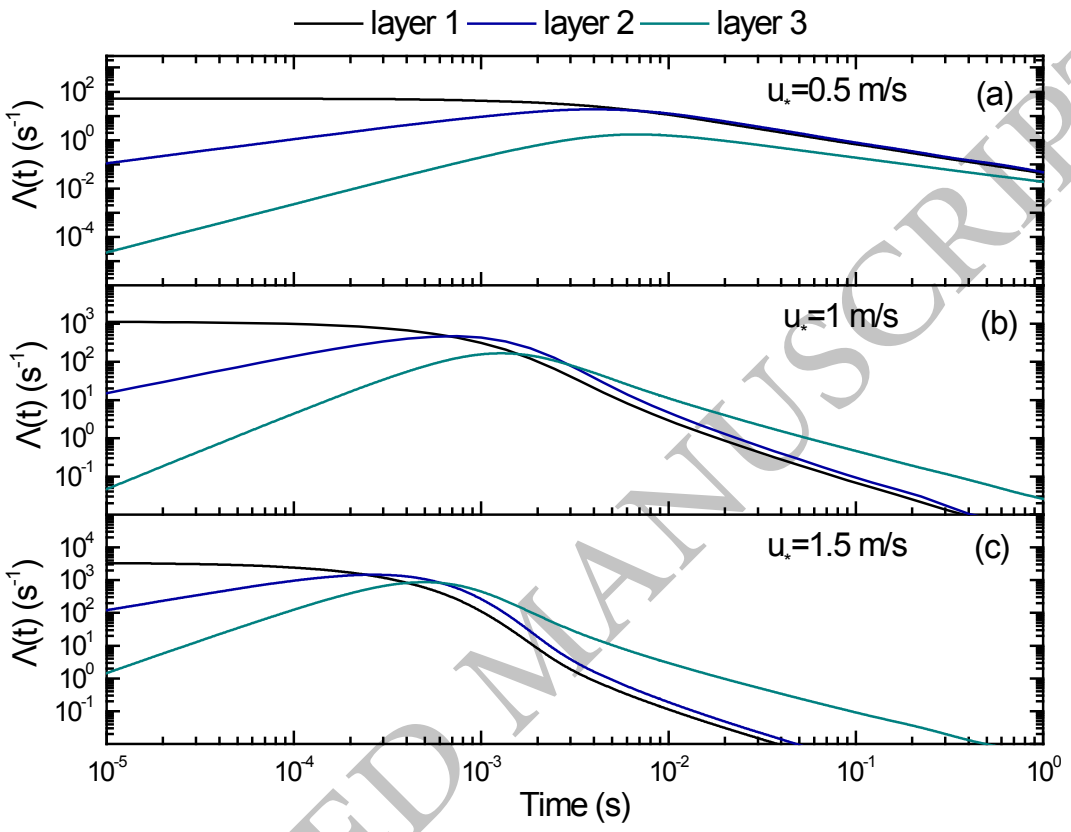

Figure 8: Fractional resuspension rate for each layer of a 3-layer deposit of 30 μm stainless steel particles on a stainless steel surface versus exposure time at different friction velocities. The *LD* kinetic was used.

Table 2: Fitted values for the decay constant using Equation (17) for each friction velocity in Figure 8.

Friction velocity, m/s	ε		
	Layer 1	Layer 2	Layer 3
0.5	1.167	1.155	1.002
1	1.710	1.686	1.372
1.5	1.829	1.805	1.547

3.5 Influence of friction velocity

Figure 9a presents the influence of friction velocity on the fractional resuspension rate, where, $\Lambda(t)$ is evaluated using three deposits that differ only on the number of the layers. It is seen that $\Lambda(t)$ increases

with u_* for low friction velocities but the opposite behaviour is observed for high friction velocities. Again, we distinguish two regimes one corresponding at low friction velocities and one corresponding at high friction velocities. Accordingly, at low-friction regime, particles resuspend with higher rates for higher friction due to the enhanced aerodynamic forces represented herein by the friction velocity. On the other hand, at high-friction regime $\Lambda(t)$ decreases with u_* since the amount of adhered particles within the deposit becomes much less than the initially deposited and the resuspension rate decreases gradually. In fact, the inset in Figure 9a indicates that peak resuspension rate corresponds to 0.5 fraction remaining for all three deposits. After that point the remaining fraction of particles is less than 50%, i.e. more particles have entrained to the air than lying within the deposit. Eventually, all particles become resuspended and $\Lambda(t)$ reaches zero values.

In agreement with the results presented in Figure 7, higher $\Lambda(t)$ was obtained from the 10-layer deposit as a result of particle resuspension from layers located at $i > 5$ initiated at 0.4 m/s. Similarly, the 5-layer deposit presents higher rates than the 3-layer deposit due to particle resuspension from layers $i > 3$.

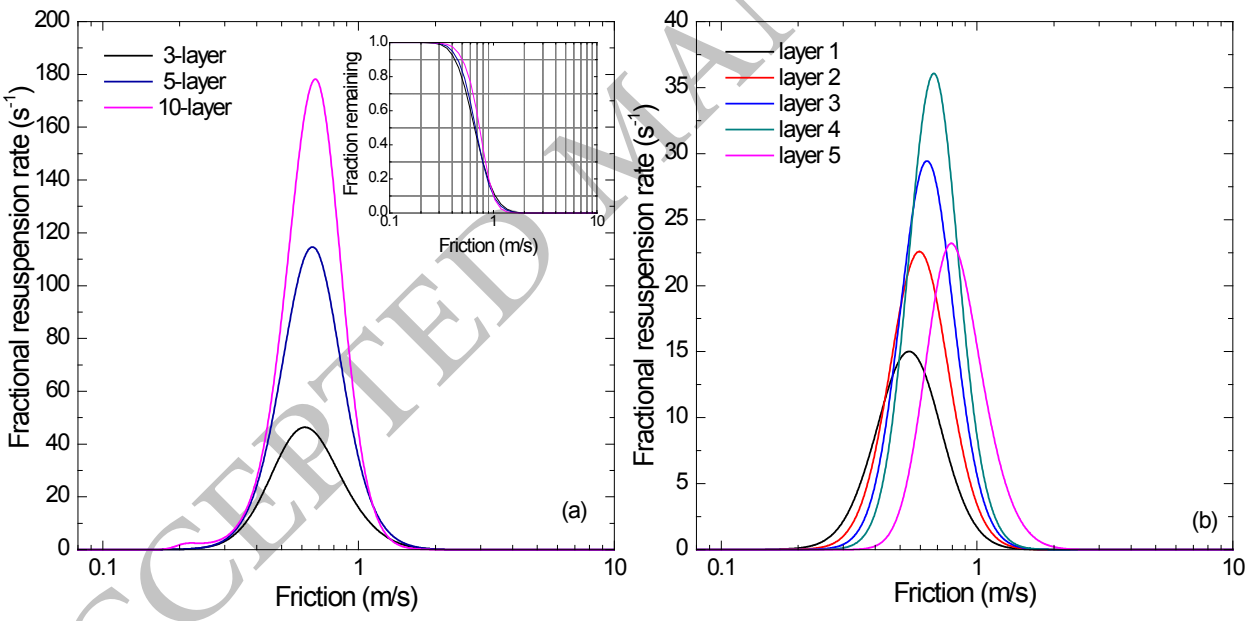

Figure 9: Fractional resuspension rate of 40 μm stainless steel particles on a stainless steel surface at $t = 0.01\,s$. a) Effect of friction velocity for a 3-layer, a 5-layer and a 10-layer deposit. The inset corresponds to the corresponding fraction remaining for each deposit. b) Effect of friction velocity in each discrete layer for a 5-layer deposit.

Moreover, Figure 9b plots $\Lambda(t)$ for each discrete layer of the 5-layer deposit presented in Figure 9a. The two regimes are indentified for all 5 layers, where at low-friction regime higher rates were obtained for

layer 1 followed gradually by the rest four layers according to their position in the deposit. However, at high-friction regime the opposite behaviour is observed and an inverse of the curves takes place. Figure 9b shows that layer 5 preserves greater $\Lambda(t)$ indicating that entrainment is dominated by particle resuspension from this layer. The remaining amount of particles available for resuspension in layer 5 is higher compared to the rest four layers, thus higher rates were obtained. On the other hand, particle entrainment from the layers 1-4 is easier due to their location in the deposit (closer to the top layer) and reduced rates were obtained as a result of less particles adhered within these layers.

4. Conclusions

A model based on a stochastic description of particle resuspension was used to evaluate single-layer resuspension rates from multilayer deposits for a range of exposure time and friction velocity. The model identifies particle resuspension from each layer using a set of kinetic equations to describe the time evolution of particle resuspension at each layer. Two kinetics were applied, the one proposed by Lazaridis and Drossinos (1998) and the one proposed by Friess and Yadigaroglu (2001), where the kinetic equations differ only in the expression for the fraction of exposed particles to the flow.

The numerical results of the present study imply minimal differences when the two kinetics were applied to a 3-layer deposit. It was demonstrated that higher fraction of exposed particles obtained by the *LD* kinetic results in increased resuspension rates compared to the *FY* kinetic only during short exposure to the airflow. On the contrary, during long exposures no difference was observed, as well as no impact of the friction velocity was found when comparing the two kinetics.

Investigation of the influence of exposure time and friction velocity to the resuspension rates confirmed the existence of two regimes for both cases. Model predictions suggest a time dependence of particle resuspension where high rates apply at short exposure (short-term regime), whereas considerably reduced rates following a power law were found at long-term regime. The two regimes were associated with the adhesive forces. In more detail, at short-term regime all weakly bound particles resuspend instantaneously, thus high rates were obtained, whereas, at long-term regime only the strong adhered particles remain in the deposit resulting in substantially reduced rates. Regarding the dependence of $\Lambda(t)$ with friction, the results demonstrate that the resuspension rate increases with u_* at low-friction regime due to the corresponding enhanced aerodynamic forces, whereas, the gradual decrease of $\Lambda(t)$ observed at high-friction regime is linked with the amount of particles remaining in the deposit (fewer particles-lower rates). In addition, an inverse of the curves of the single-layer resuspension rates was obtained at long-term and high-friction regimes. This behaviour was associated in both cases with the growth of resuspension within

the deposit and the relevant dominant layer. Under these circumstances, it was demonstrated that the position of the layer within the deposit plays an important role at the evolution of the process both in terms of a long exposure to the flow and for enhanced aerodynamic forces.

Acknowledgments

This work was supported by the European Union 7th framework program HEXACOMM FP7/2007-2013 under grant agreement Nº 315760.

References

Barth, T., Reiche, M., Banowski, M., Oppermann, M., Hampel, U., (2013). Experimental investigation of multilayer particle deposition and resuspension between periodic steps in turbulent flows. *J. Aerosol Sci.*, 64:111-124.

Benito, J. G., Valenzuela Aracena, K. A., Uñac, R. O., Vidales, A. M., and Ippolito, I., 2015. Monte Carlo modelling of particle resuspension on a flat surface. *J. Aerosol Sci.*, 79:126-139.

Boor, B.E., Siegel, J.A., Novoselac, A., (2013a). Monolayer and multilayer particle deposits on hard surfaces: Literature review and implications for particle resuspension in the indoor environment. *Aerosol Sci. Technol.*, 47:831-847.

Boor, B.E., Siegel, J.A., Novoselac, A., (2013b). Wind tunnel study on aerodynamic particle resuspension from monolayer and multilayer deposits on linoleum flooring and galvanized sheet metal. *Aerosol Sci. Technol.*, 47: 848-857.

Chatoutsidou S.E., Drossinos Y., Tørseth H., Lazaridis M., (2016). Modelling of particle resuspension by a turbulent airflow and the role of particle size, surface roughness and electric charge. Journal of Adhesion Science and Technology 2016, DOI: 10.1080/01694243.2016.1232955.

Friess, H., Yadigaroglu, G. (2001). A generic model for the resuspension of multilayer aerosol deposits by turbulent flow. *Nucl Sci Eng*, 138:161-176.

Friess, H., Yadigaroglu, G. (2002). Modeling of the resuspension of particle clusters from multilayer aerosol deposits with variable porosity. *J. Aerosol Sci.*, 33:883-906.

Fromentin, A. (1989). Particle resuspension from a multi-layer deposit by turbulent flow. Ph.D. thesis. Swiss Federal Institute of Technology, Zurich.

Goldasteh, I., Ahmandi, G., and Ferro., A. R. (2013). Monte Carlo simulation of micron size spherical particle removal and resuspension from substrate under fluid flows. *J. Aerosol Sci.*, 66:62-71.

Guingo, M., and Minier, J.-P. (2008). A new model for the simulation of particle resuspension by turbulent flows based on a stochastic description of wall roughness and adhesion forces. *J. Aerosol Sci.*, 39:957-973.

Henry C, Minier J-P. Progress in particle resuspension from rough surfaces by turbulent flows.*Prog.Energy Combust. Sci*. 2014;45:1-53.

Ibrahim, A. H., Dunn, P. F., and Brach, R. M. (2003). Microparticle detachment from surfaces exposed to turbulent air flow: controlled experiments and modelling. *J. Aerosol Sci.*, 34:765-782.

Lazaridis, M., and Drossinos, Y. (1998). Multilayer resuspension of small identical particles by turbulent flow. *Aerosol Sci. Technol.*, 28:548-560.

Lazaridis, M., Drossinos, Y., and Georgopoulos, P.G., (1998). Turbulent resuspension of small Nonderfomable Particle. *J. Colloid Interface Sci.*, 204:24-32.

Lecrivain, G., Vitsas, A., Boudounis, A.G., Hampel, U. (2014). Simulation of multilayer particle resuspension in an obstructed channel flow. *Powder Technology*, 263, 142-150.

Leighton, D., and Acrivos, A. (1985). The lift on a small sphere touching a plane in the presence of a simple shear flow. *Journal of Applied Mathematics and Physics*, 36:174-178.

Mukai C., Siegel G.A., Novoselac A. (2009). Impact of airflow characteristics on particle resuspension from indoor surfaces. *Aerosol Sci. Techno*., 43:10, 1022-1032.

O'Neil, M. E. (1968). A sphere in contact with a plane wall in a slow linear shear flow. *Chem. Eng. Sci.*, 23:1293-1298.

Reeks, M. D., and Hall, D. (2001). Kinetic models for particle resuspension in turbulent flows: theory and measurement. *J. Aerosol Sci.*, 32:1-31.

Reeks, M. W., Reed, J., and Hall., D. (1988). On the resuspension of small particles by a turbulent flow. *J. Phys. D: Appl. Phys.*, 21:574-589.

Stempniewicz M.M., Komen E.M.J., de With A. (2008). Model of particle resuspension in turbulent flows. *Nuclear Energy and Design*, 238:2943-2959.

Wang, S., Zhao, B., Zhou, B., Tan, Z., (2012). An experimental study on short-time particle resuspension from inner surfaces of straight ventilation ducts. *Build. Environ.*, 53:119-127.

Wen, H. Y., Kasper, G., (1989). On the kinetics of particle re-entrainment from surfaces. *J. Aerosol Sci,* 20:483-498.

Wu, Y.-L., Davidson, C. I., Russell, A. G., (1992). Controlled wind tunnel experiments for particle bounceoff and resupension. *Aerosol Sci. Technol.*, 17:245-262.

Zhang, F., Reeks, M. W., Kissane, M. P., Perkins, R. J. (2013). Resuspension of small particles from multilayer deposits in turbulent boundary layers. *J. Aerosol Sci.*, 66:31-61.

Zhou, B., Zhao, B., Tan, Z., (2011). How particle resuspension from inner surfaces of ventilation ducts affects indoor air quality-A modelling analysis. *Aerosol Sci. Techno.,* 45:996-1009.

Ziskind, G., Fichman, M., and Gutfinger, C. (1995). Resuspension of particulates from surfaces to turbulent flows-Review and analysis. *J. Aerosol Sci.*, 26:613-644.

Ziskind, G., Fichman, M., and Gutfinger, C. (1997). Adhesion moment model for estimating particle detachment from a surface. *J. Aerosol Sci.*, 28:623-634.

Ziskind, G. (2006). Particle resuspension from surfaces: Revisited and re-evaluated. *Reviews in Chemical Engineering*, 22:1-123.